Natural Resources Canada / Ressources naturelles Canada

GEOLOGICAL SURVEY OF CANADA
OPEN FILE 7744

Mapping Hydrothermal Footprints: Case Studies from the Meliadine Gold District, Nunavut

C.J.M. Lawley, B. Dubé, P. Mercier-Langevin, and D. Vaillancourt

2015

Canada

GEOLOGICAL SURVEY OF CANADA
OPEN FILE 7744

Mapping Hydrothermal Footprints: Case Studies from the Meliadine Gold District, Nunavut

C.J.M. Lawley[1], B. Dubé[2], P. Mercier-Langevin[2], and D. Vaillancourt[3]

[1]Natural Resources Canada, Geological Survey of Canada, 601 Booth Street, Ottawa, Ontario
[2]Ressources naturelles Canada, Commission géologique du Canada, 490 rue de la Couronne, Québec, Québec
[3]Agnico-Eagle Mines Limited, 765 chemin de la Mine Goldex, Val D'Or, Québec

2015

doi:10.4095/295920

Recommended citation
Lawley, C.J.M., Dubé, B., Mercier-Langevin, P., and Vaillancourt, D., 2015. Mapping hydrothermal footprints: Case studies from the Meliadine gold district, Nunavut; Geological Survey of Canada, Open File 7744, 22 p. doi:10.4095/295920

Publications in this series have not been edited; they are released as submitted by the author.

Mapping Hydrothermal Footprints: Case studies from the BIF-hosted Meliadine Gold District, Nunavut

Lawley*, C.J.M.[1], Dubé, B.[2], Mercier-Langevin, P.[2], and Vaillancourt, D.[3]
(1) Natural Resources Canada, Geological Survey of Canada, 601 Booth Street, Ottawa, Ontario
(2) Ressources naturelles Canada, Commission géologique du Canada, 490 rue de la Couronne, Québec, Québec
(3) Agnico-Eagle Mines Limited, 765 Chemin de la mine Goldex, Val D'Or, Québec
*clawley@NRCan.gc.ca

The geochemical and mineralogic signature, or hydrothermal footprint, of ore deposits has great potential as an exploration tool. In some cases, hydrothermal footprints can be mapped up to several kilometers beyond the economically viable portion of the deposit and thus offers the potential to vector from sub-economic mineralization towards higher-grade ore from district- to deposit-scales. Conventionally, hydrothermal footprints are mapped using some preferred threshold concentration for each pathfinder element, or ratio, of interest. The results are then generally portrayed as stacked geochemical traverses adjacent to known ore bodies. However, the conventional approach inadequately accounts for the multivariate nature of ore processes and the inherently imprecise boundary between barren and mineralized rock. In this contribution we explore alternative methods to define and map the hydrothermal footprint at six gold deposits and ore zones within the Meliadine Gold District (MGD), Nunavut.

MGD host rocks are variably altered (silicified ± sericitized ± sulphidized ± carbonatized ± chloritized) adjacent to BIF-hosted replacement-style gold mineralization and auriferous greenstone-hosted quartz (± ankerite) veins cutting mafic volcanic, interflow sediments and turbiditic successions. Robust principle component analysis defines key element assemblages (Au-Ag-As-S-Te-Bi-W-Sb) that are associated with gold and are enriched from 10s to 100s of meters adjacent to ore zones. We integrate and map pathfinder element enrichment and quantified measures of hydrothermal alteration intensity using a hybrid fuzzy- and conditional probability-based model (weights of evidence) in an effort to further highlight the complementary nature of multivariate datasets and to define fuzzy footprints. The available whole-rock data suggests that multi-element anomalies are, in some instances, better suited for defining broader geochemical anomalies than was apparent from analysis of individual pathfinder elements. We emphasize that samples containing pathfinder element concentrations in excess of some preferred threshold are akin to conventional definitions of geochemical anomalies, but in this case occur primarily in the ore zone and are thus of limited use for vectoring. In contrast, fuzzy footprints delineate the simultaneous occurrence of favourable pathfinder element enrichment and hydrothermal alteration for samples that would have been excluded following the conventional approach. These samples occur in hanging wall and footwall rocks devoid of gold ($<$ 5 ppb), and thus provide a possible vector to high-grade gold ore.

Slide 1

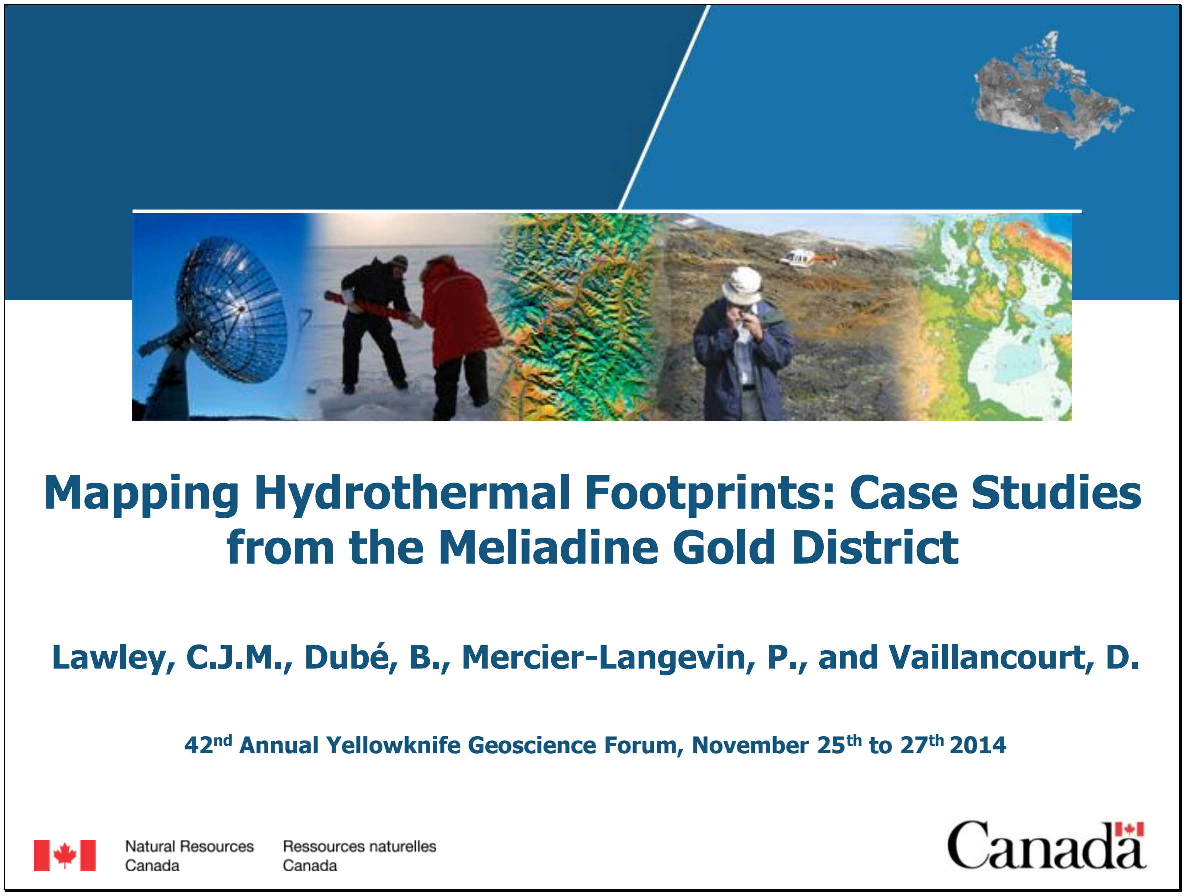

Herein we report the results of one study completed as part of the Targeted Geoscience Initiative (TGI)-4 program at the Meliadine Gold District, Nunavut, Canada.

Slide 2

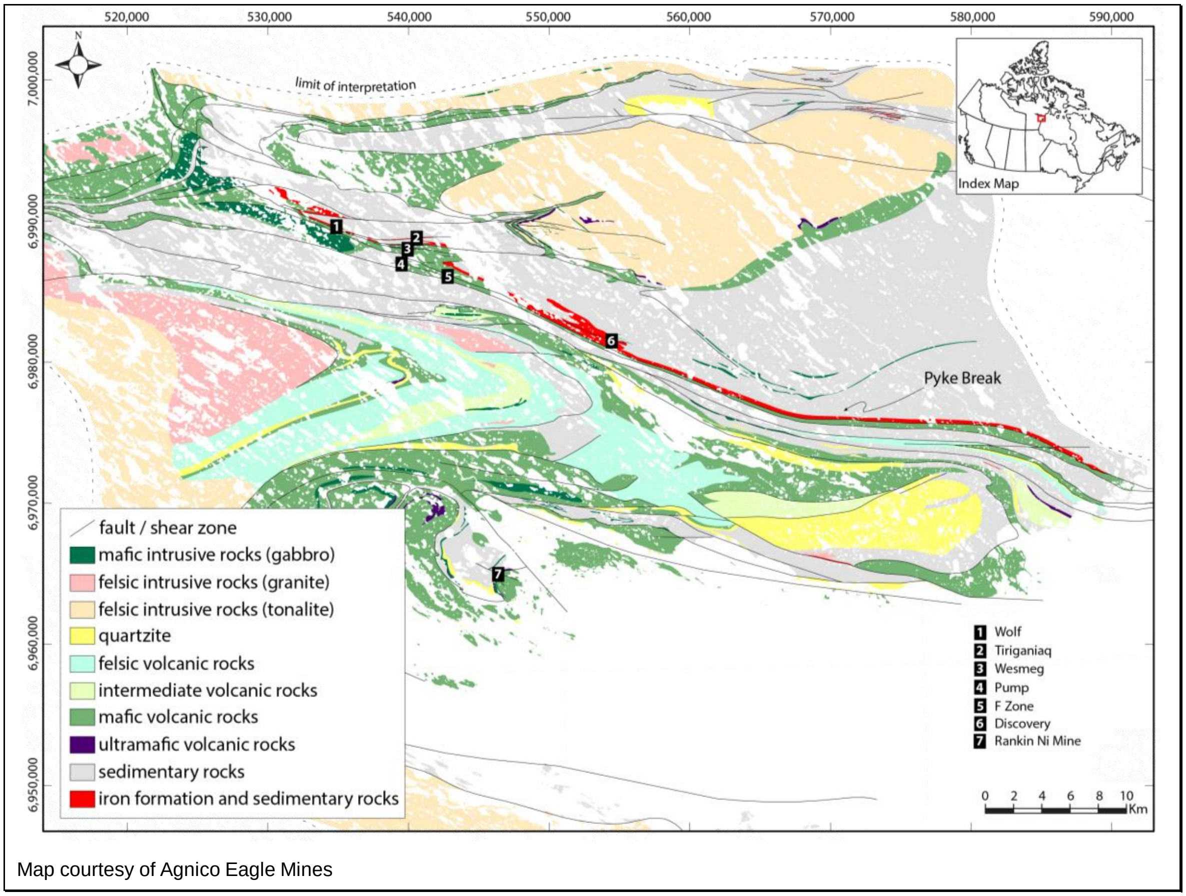

Local geological map of the Meliadine Gold District (map courtesy of Agnico Eagle Mines). The largest of the known gold deposits occur along the Pyke Break (Wolf, Tiriganiaq, Wesmeg, Pump, F Zone, and Discovery). Rankin Inlet and the former Rankin Ni Mine are shown for reference.

Slide 3

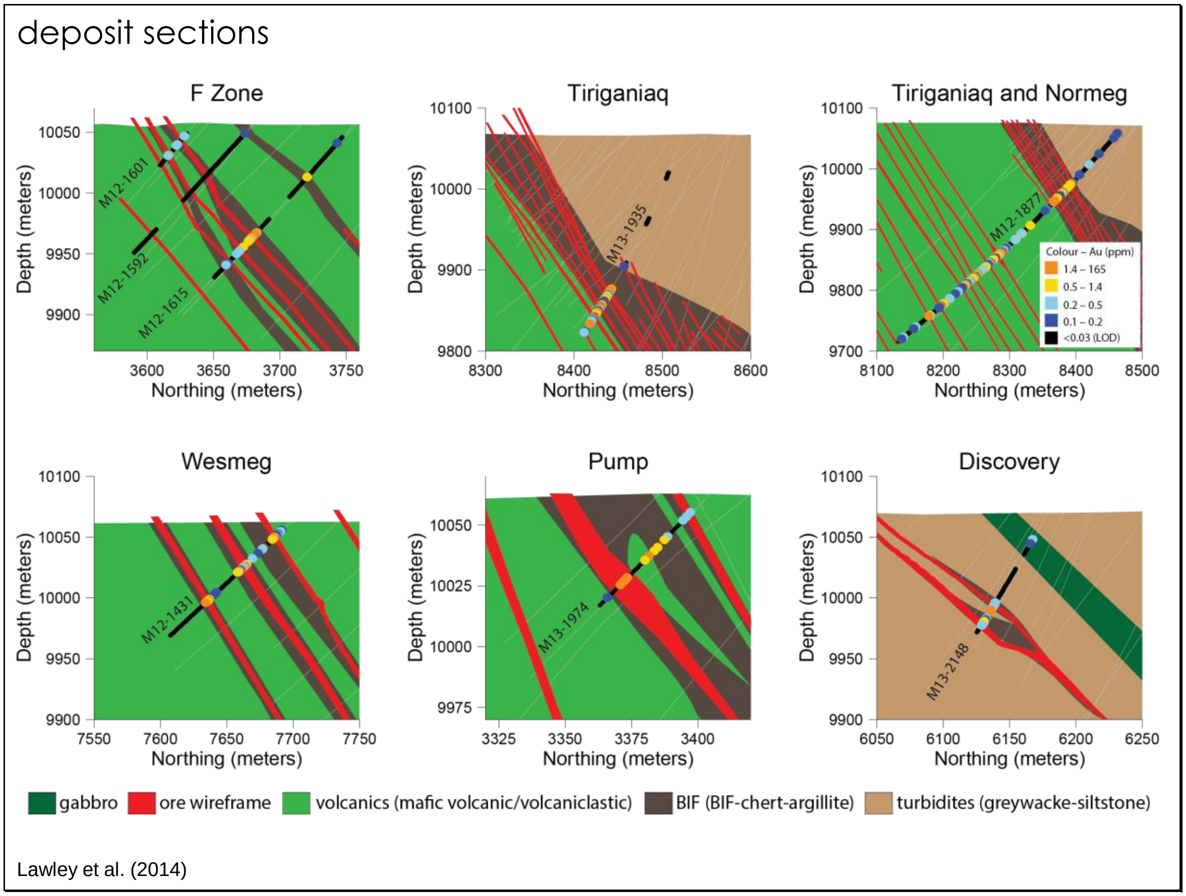

Simplified sections show the simplified geology and ore resource wireframes from 3D modelling at each deposit. Agnico Eagle Mines gold fire assays, after dividing into quartiles, are plotted alongside the trace of each of borehole. Note that ore wireframes are not gold-rich along their entire strike length or dip extent. Gold concentrations rarely exceed the LOD in the deposit's hanging wall and footwall. Deposit host rocks are subdivided into four lithofacies: (1) volcanic; (2) Banded Iron Formation (BIF); (3) turbidite; and (d) dikes (sections are shown using an Agnico Eagle mine grid).

Slide 4

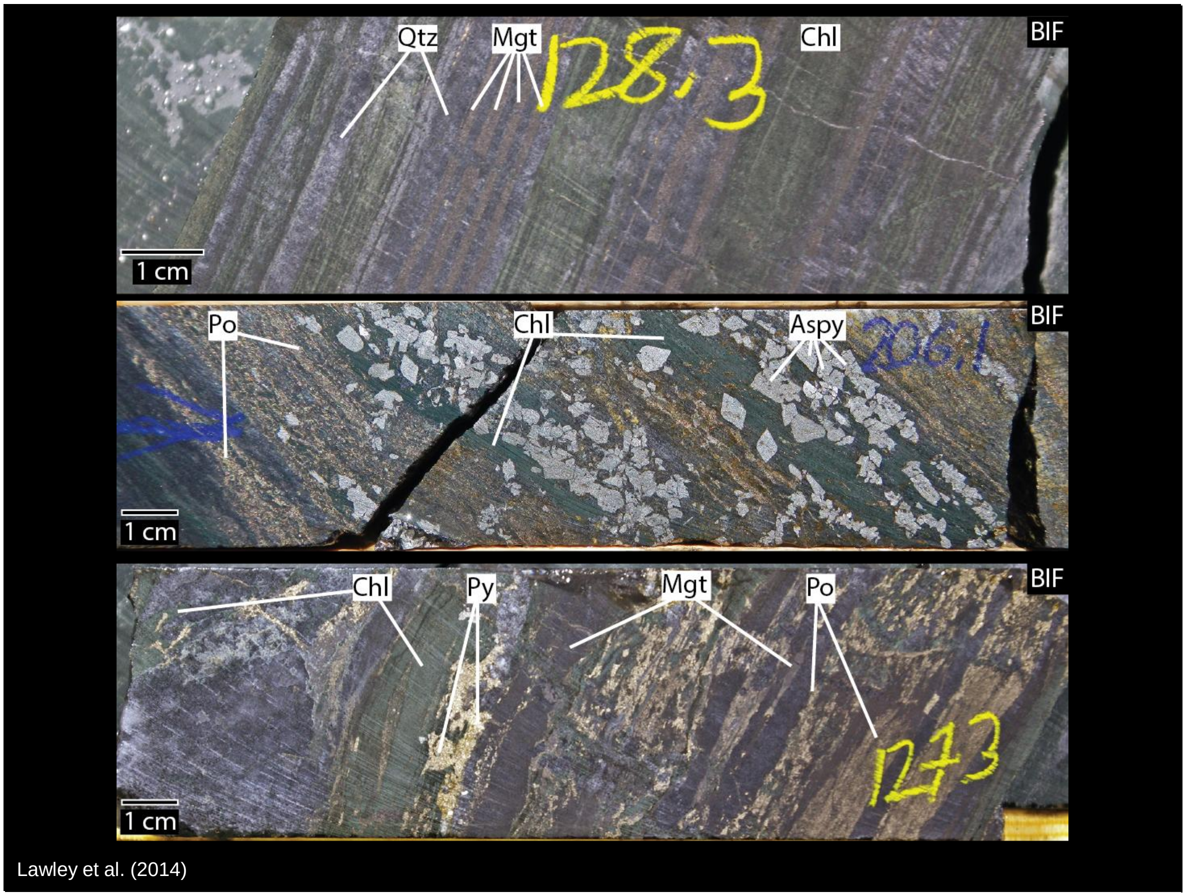

Core photos of variably altered BIF (abbreviations: Aspy = arsenopyrite; Py = pyrite; Mgt = magnetite; Qtz = quartz; Chl = chlorite; Po = pyrrhotite)

Slide 5

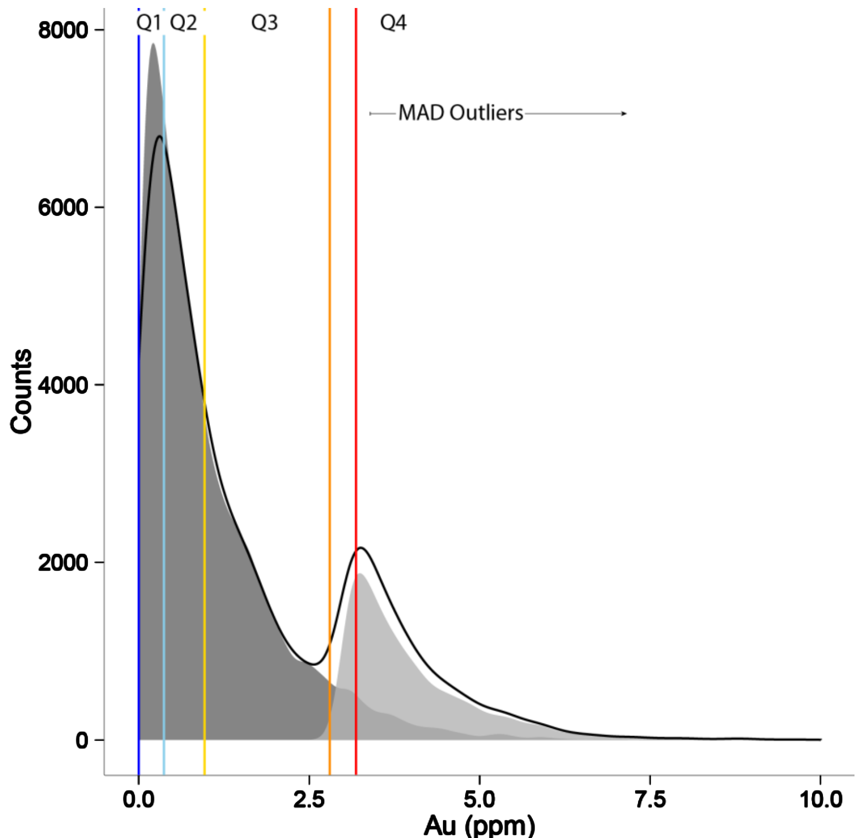

Lawley et al. (2014)

Synthetic log-normal density distribution functions for background (dark grey) and mineralized (light grey) sub-populations. The density distribution functions for both sub-populations are shown as a black line. Vertical lines correspond to the Median Absolute Deviation (MAD) outlier threshold and quartiles (Q1–Q4) for the entire synthetic dataset. The simulation highlights the challenge of separating background from mineralized sample populations even for synthetic cases where the compositional characteristics of both sub-populations are precisely known. In practice, the distinction between barren and mineralized samples is imprecisely known, or fuzzy.

Slide 6

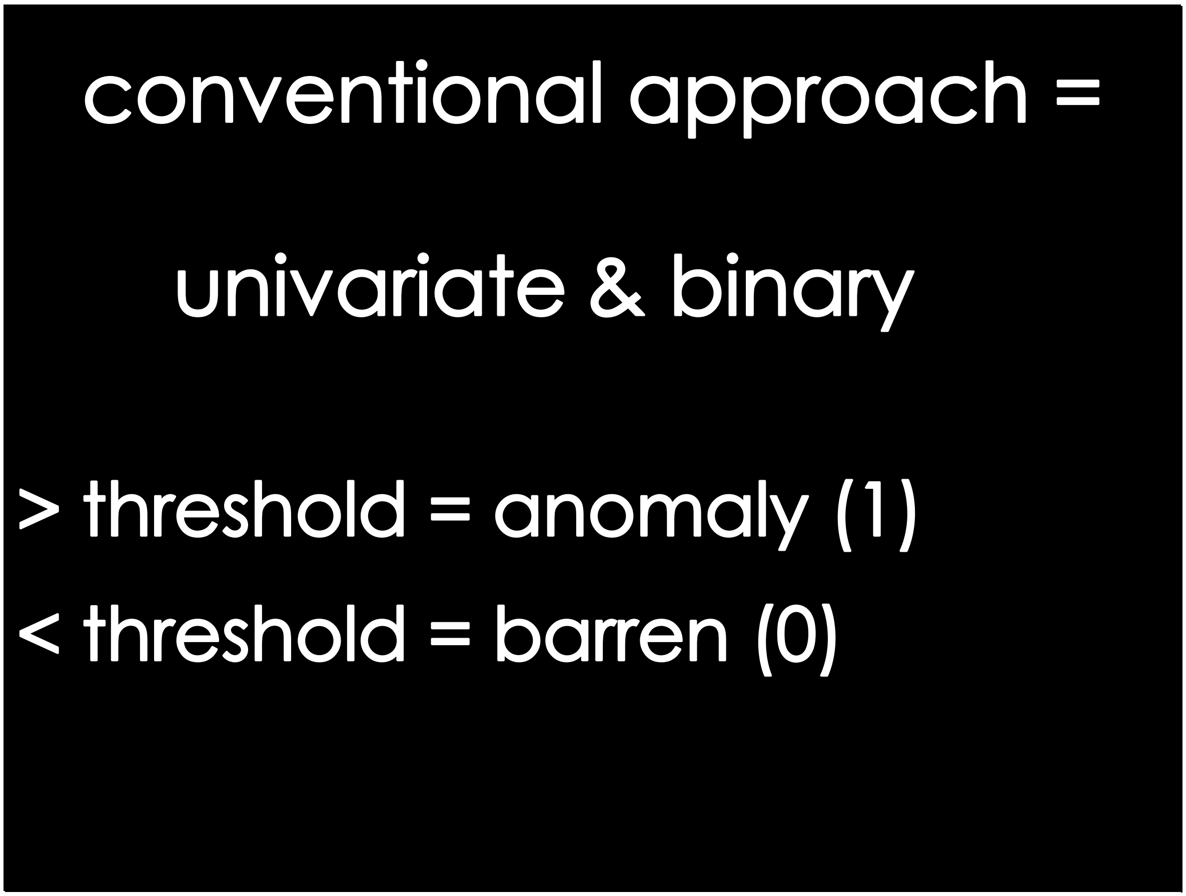

Conventionally, rocks are subdivided into anomalous and non-anomalous sample sets using some qualitative or statistically-defined threshold, typically on an element-by-element basis. This approach is unsatisfactory for at least two reasons: (1) ore deposits represent multi-element geochemical anomalies. For example, gold is a key element of economic interest at a variety of ore deposit types, but most often occurs along with a diverse element suite of lesser economic interest that can, at least locally, extend beyond gold ore (i.e., pathfinder elements). Geochemical anomaly mapping thus requires a multivariate approach; and (2) geochemical anomalies, based on binary definitions (i.e., defining anomalies as true or false; 1 or 0), are inadequate to classify rocks that are not clearly barren or mineralized. Effective hydrothermal footprint vectoring rests with the appropriate handling of these transitional samples.

Slide 7

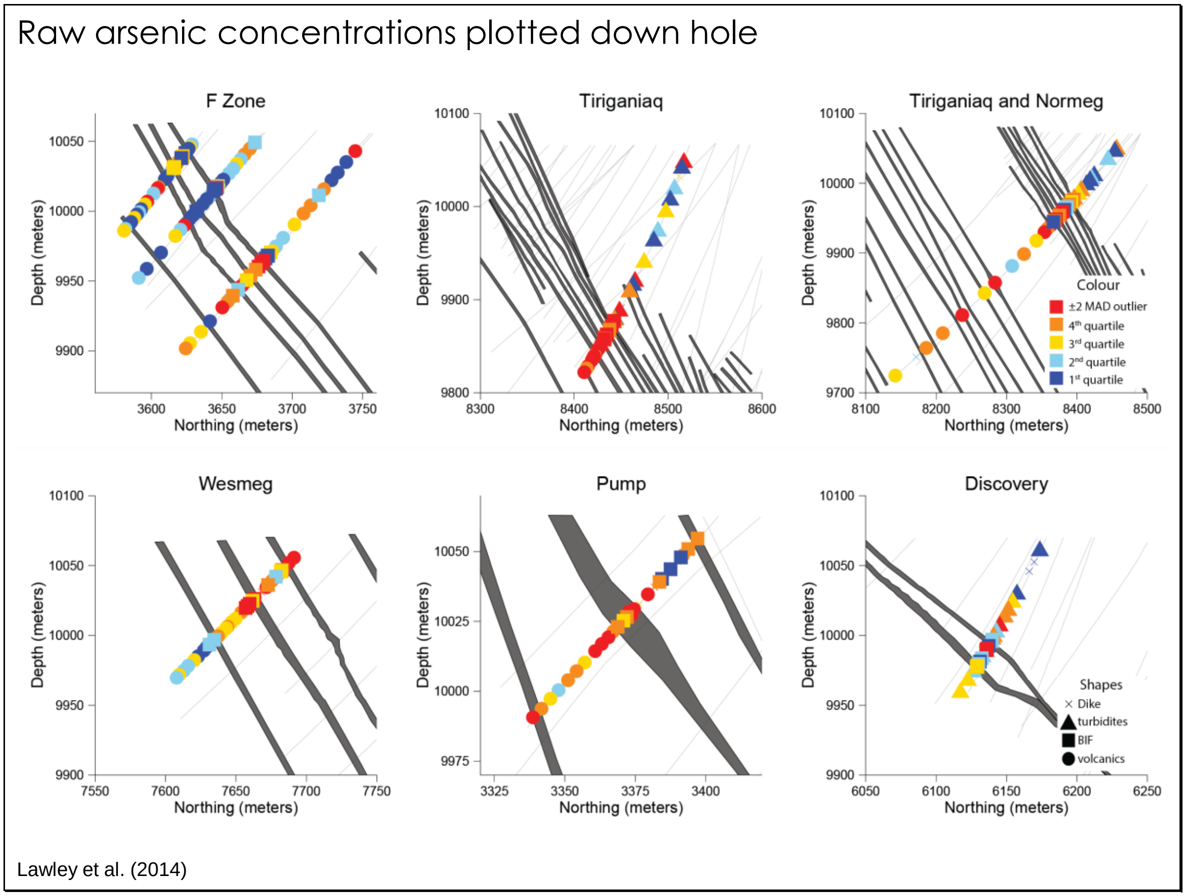

Raw As concentrations following MAD outlier and quartile subdivision for each lithofacies. Ore wireframes (grey polygons) and borehole traces are shown for reference. The data demonstrates that BIF-hosted replacement-style gold ore is associated with MAD As outliers. Hanging wall and footwall rocks devoid of gold (≤ 5 ppb) are enriched in As (Q4 ± Q3). Geochemically anomalies adjacent to ore zones extend for 100s to 10s of meters at Normeg and the other deposits, respectively (sections shown with mine grid).

Slide 8

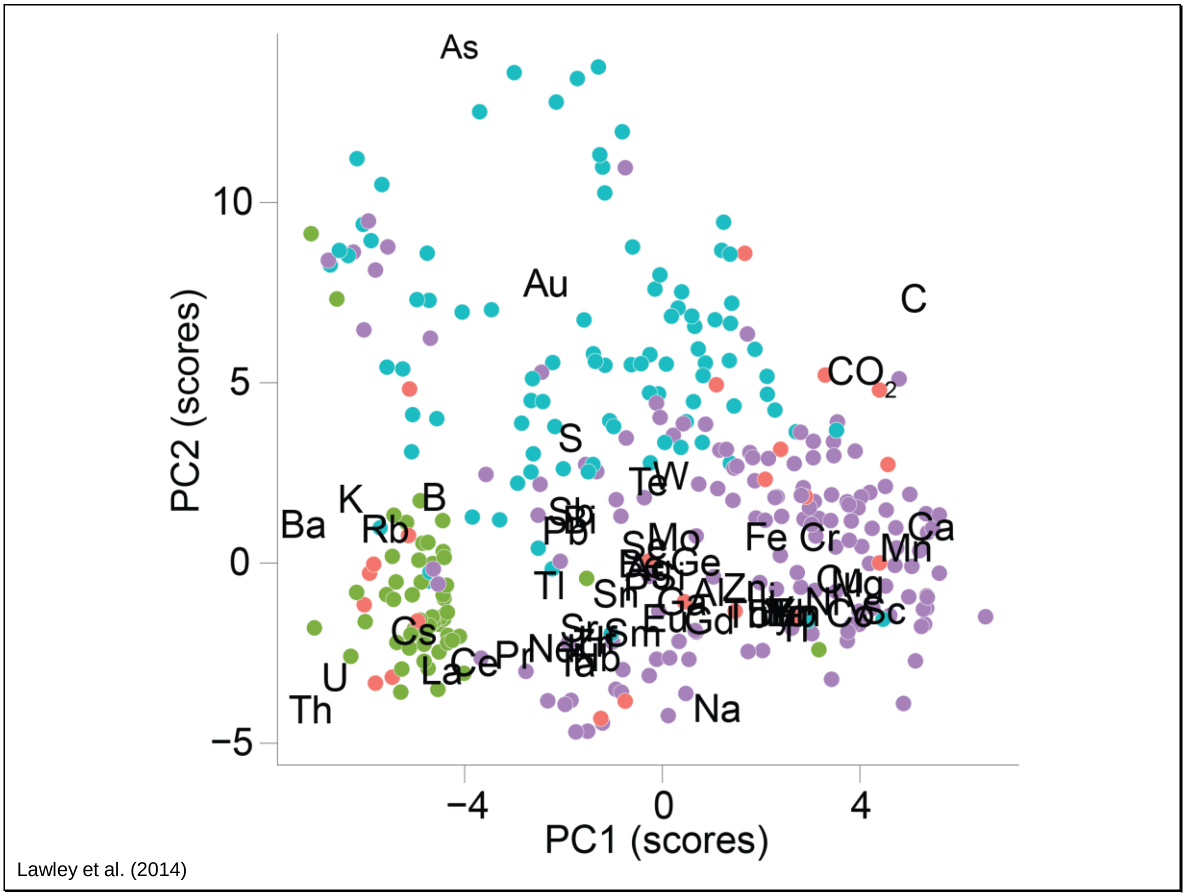

Ore deposits represent multi-element geochemical anomalies. Robust Principal Components Analysis (PCA) bi-plot showing PCA scores and loadings for PC1–PC3. PC2 yields high-loadings for As-Au-S-Sb-Bi-Te-W and suggests that this principal component can be used to map this multi-element ore signature at the MGD. Data-points are colour coded according to lithofacies (blue = BIF; purple = volcanic; green = turbidite; red = dike).

Slide 9

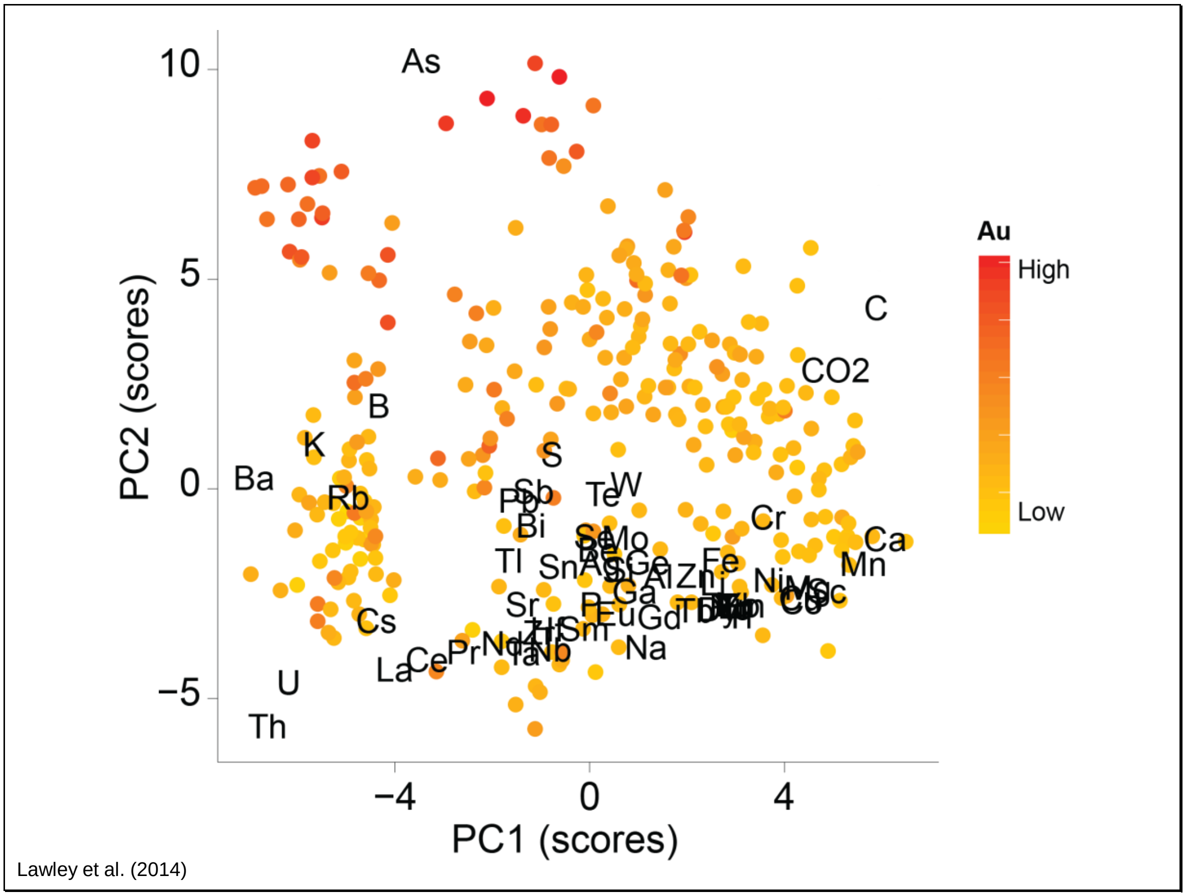

Robust PCA biplot after excluding gold. Sample points are colour coded to gold concentration (yellow = gold poor; red = gold rich) and show that PC2 scores remains a relatively good indicator of gold grade, due primarily, to high loadings for As even after excluding gold from the PCA

Slide 10

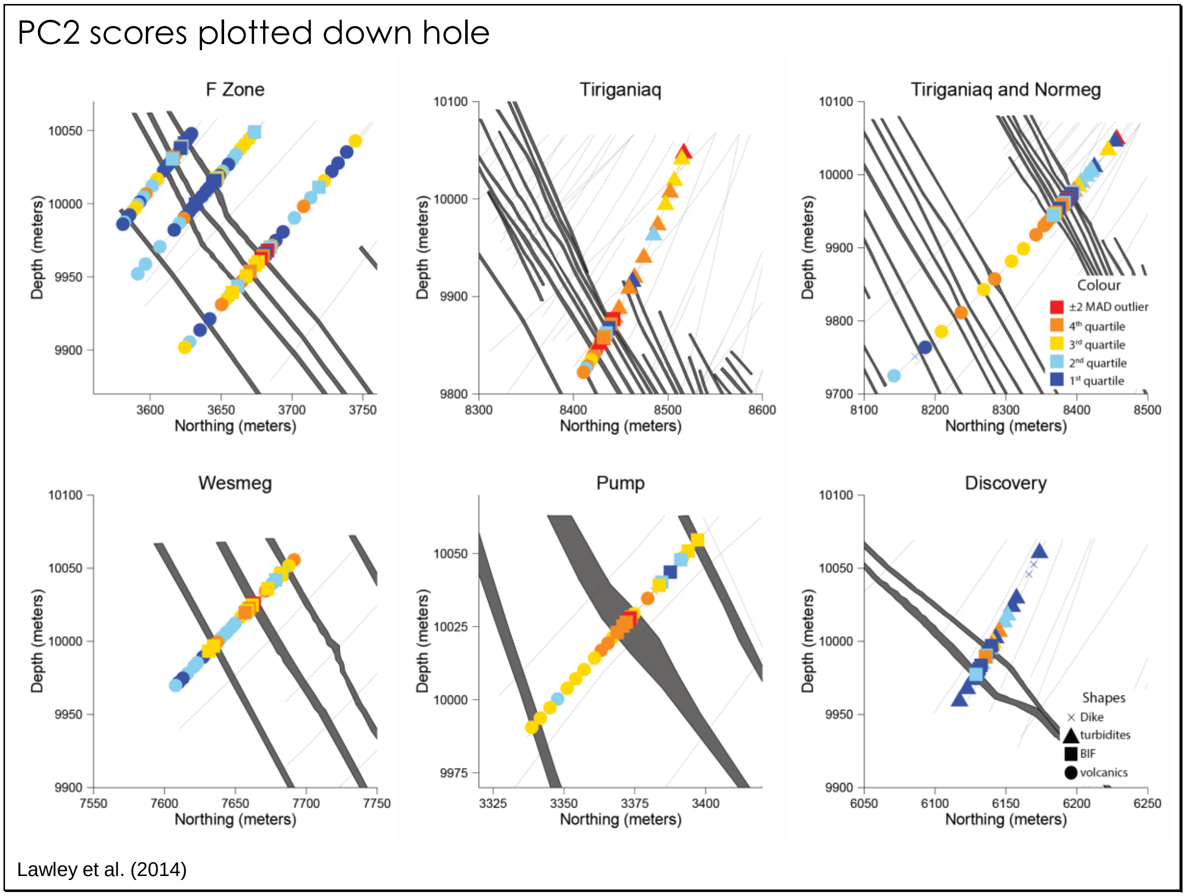

PC2 scores plotted down hole are colour coded to quartiles after excluding MAD outliers and calculated for each lithofacies. The data shows that anomalous and elevated (Q4 ± Q3) PC2 scores are co-spatial with BIF-hosted replacement style gold mineralization. Elevated PC2 scores also extend at least 200 m into hanging wall rocks devoid of gold (<5 ppb) at Tiriganiaq; whereas the multi-element halo at Wesmeg appears to possess a more restricted distribution. An apparent progression from un-mineralized wall rock to gold ore is observed at Discovery.

Slide 11

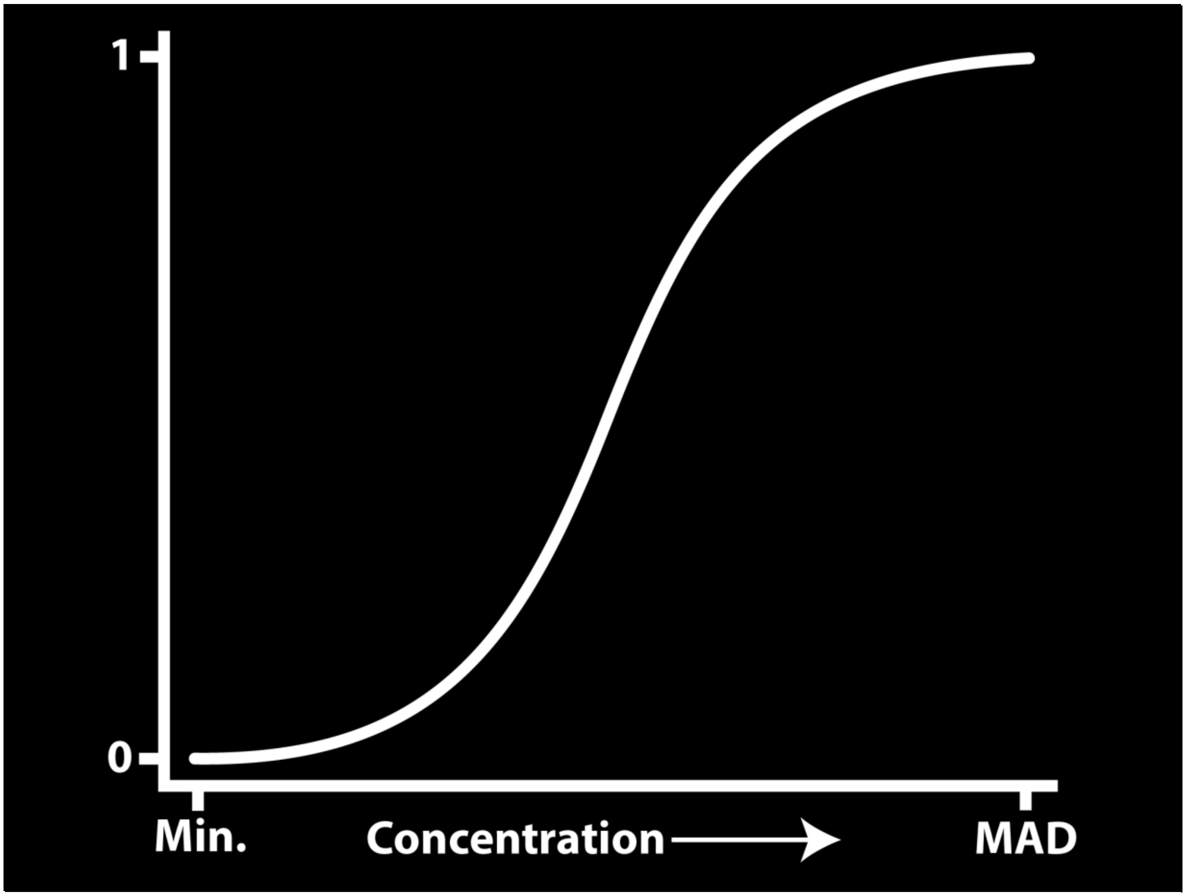

Hydrothermal footprints are conventionally mapped using a binary anomaly definition (i.e., True or False). Multi-valued logic frameworks provide an alternative approach. Herein we consider concentrations outside of the median ± 2 Median Absolute Deviations [MAD; MAD = median(|Xi – median (Xi)|), where the values in brackets represent absolute differences between the sample values and their median] as anomalous and are given a value of 1. Whereas, the data minimum is assigned a value of 0. All other concentrations are assigned a number between 0 and 1 based on an S-shaped function. This approach emphasizes concentrations close to the MAD threshold for each element and corrects, to some extent for geochemical differences between rock types.

Slide 12

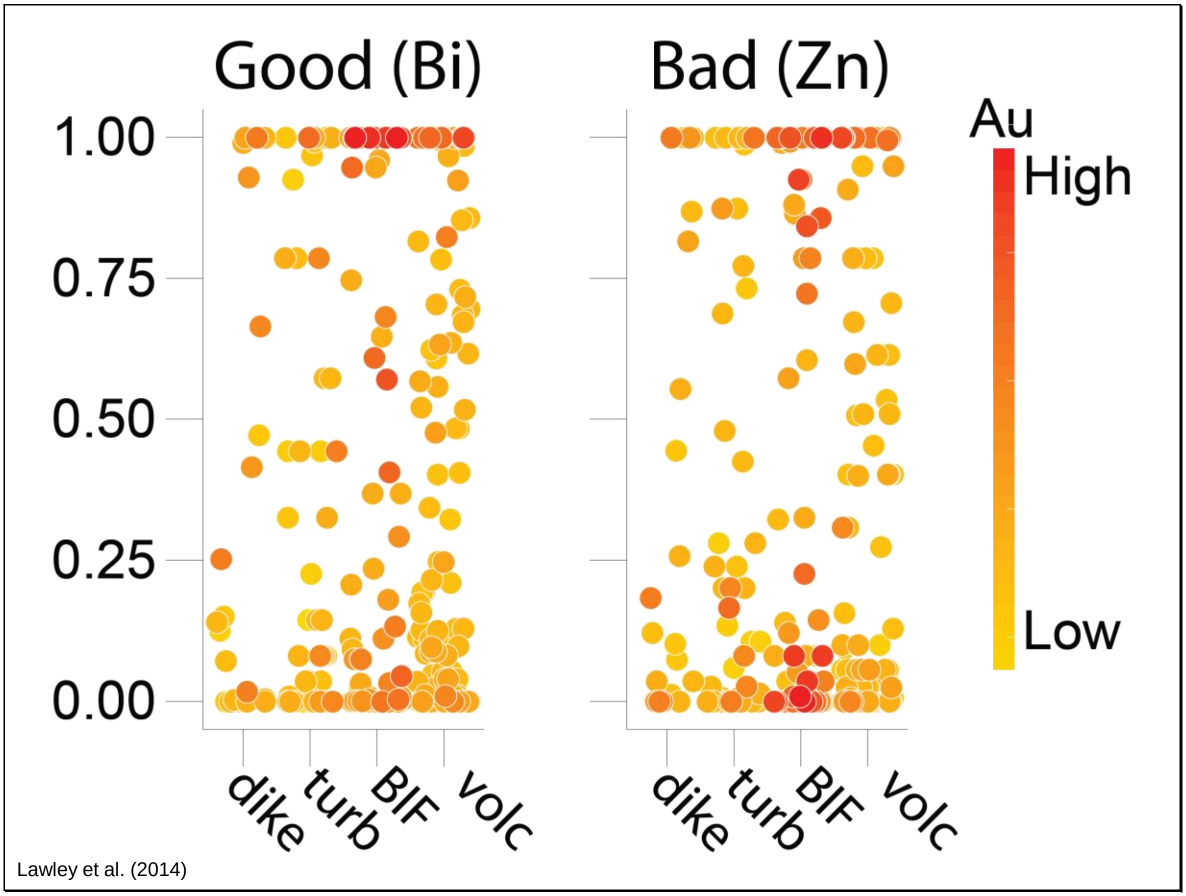

The relationship between pathfinder element concentration, reassigned following an S-shaped membership function, and gold can be visualized on dot plots. S-shaped memberships (y axis) for each sample are colour coded to gold concentration and subdivided according to lithofacies (x axis; turb = turbidite; volc = volcanic) for each combination. Useful pathfinder elements yield S-shaped memberships that correctly correspond to gold-rich samples (red dots plot close to 1). Less effective pathfinder elements are recognized by gold-rich samples with low S-shaped memberships (red dots plot close to 0).

Slide 13

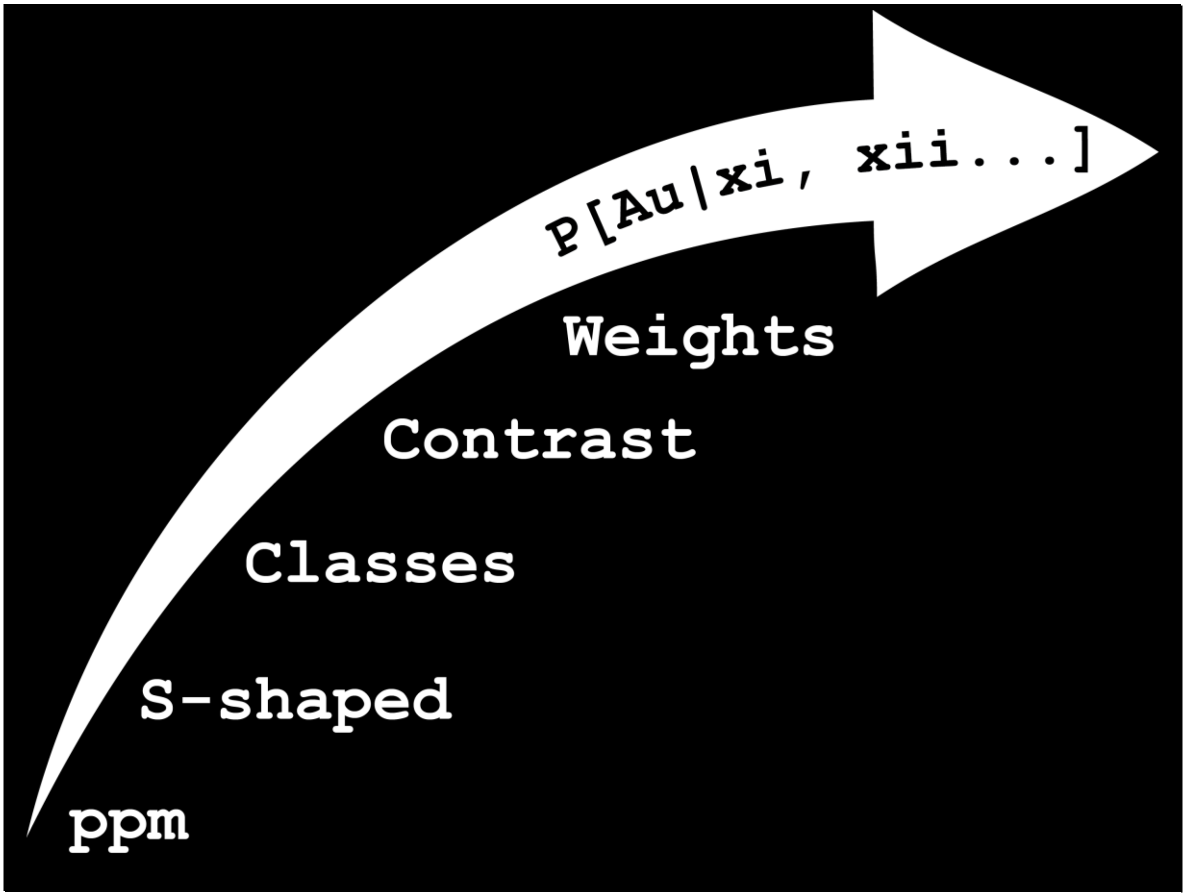

Herein we addressed the fuzzy nature of hydrothermal footprints by following a fuzzy Weights of Evidence (WofE) approach (Cheng and Agterberg, 1999). First, raw trace element concentrations (ppm) were re-classified using an S-shaped membership function for each lithofacies. Re-classified S-shaped values were then split into five classes for each element (>MAD and Q4 to Q1). The spatial association between each class and gold (i.e., contrast value; Cheng and Agterberg, 1999) were calculated for each class and subsequently used to assign fuzzy weights. This approach differs from conventional WofE where anomalies are considered to be true or false. Finally, the weights of element classes with the strongest spatial-relationship to gold were used to calculate the posterior probabilities for each sample under the assumption of conditional independence.

Slide 14

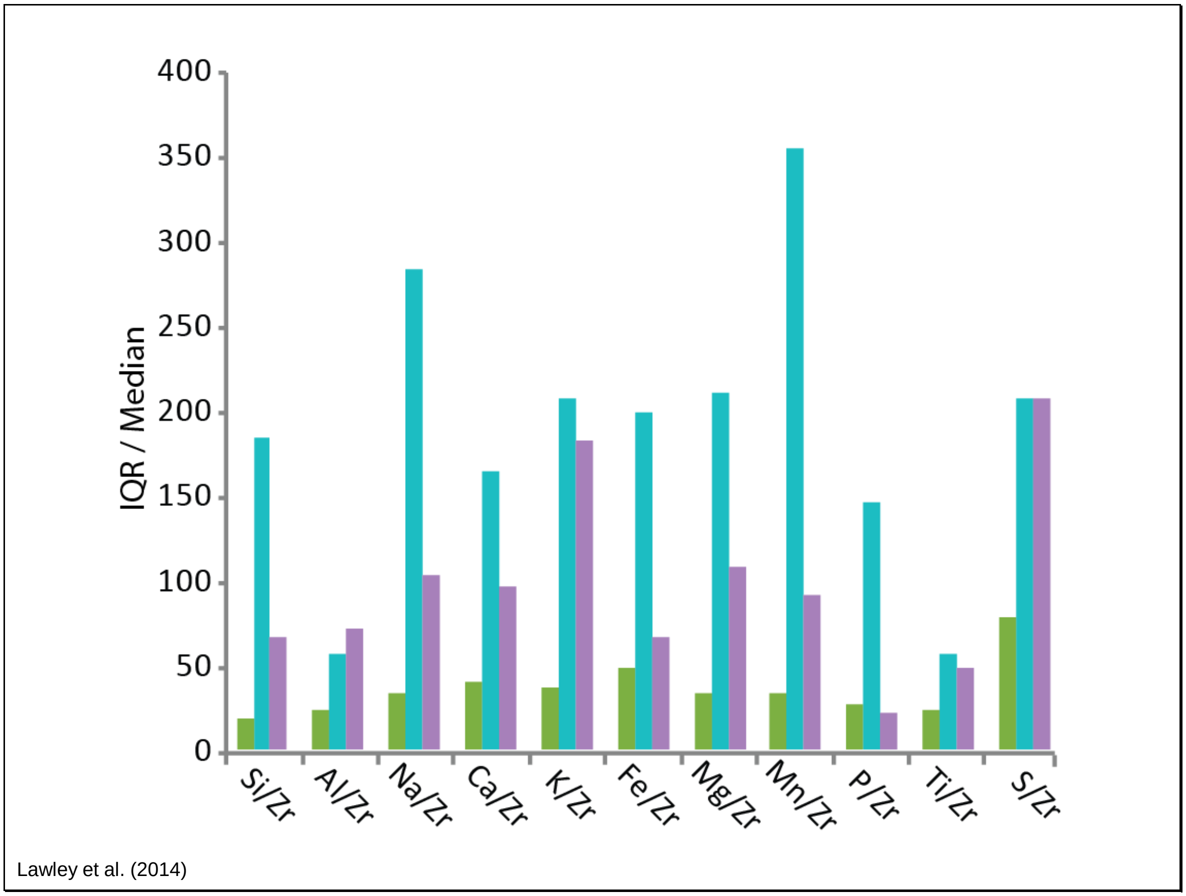

Bar plot showing Pearce Element Ratio (PER) variability [measured here as the inter-quartile range (IQR) divided by the median] subdivided according to lithofacies (green = turbidite; blue = volcanic; purple = BIF). PERs with small variation likely acted, by definition, as immobile elements; whereas heterogeneous PERs may have participated in material hydrothermal alteration. In all cases, BIF and volcanic PERs yield the most variation, whereas turbidites record relatively little evidence for hydrothermal alteration. Fuzzy WofE (Cheng and Agterberg, 1999) were also calculated for simple PERs and integrated with pathfinder element enrichment in order to map the fuzzy footprint at the MGD.

Slide 15

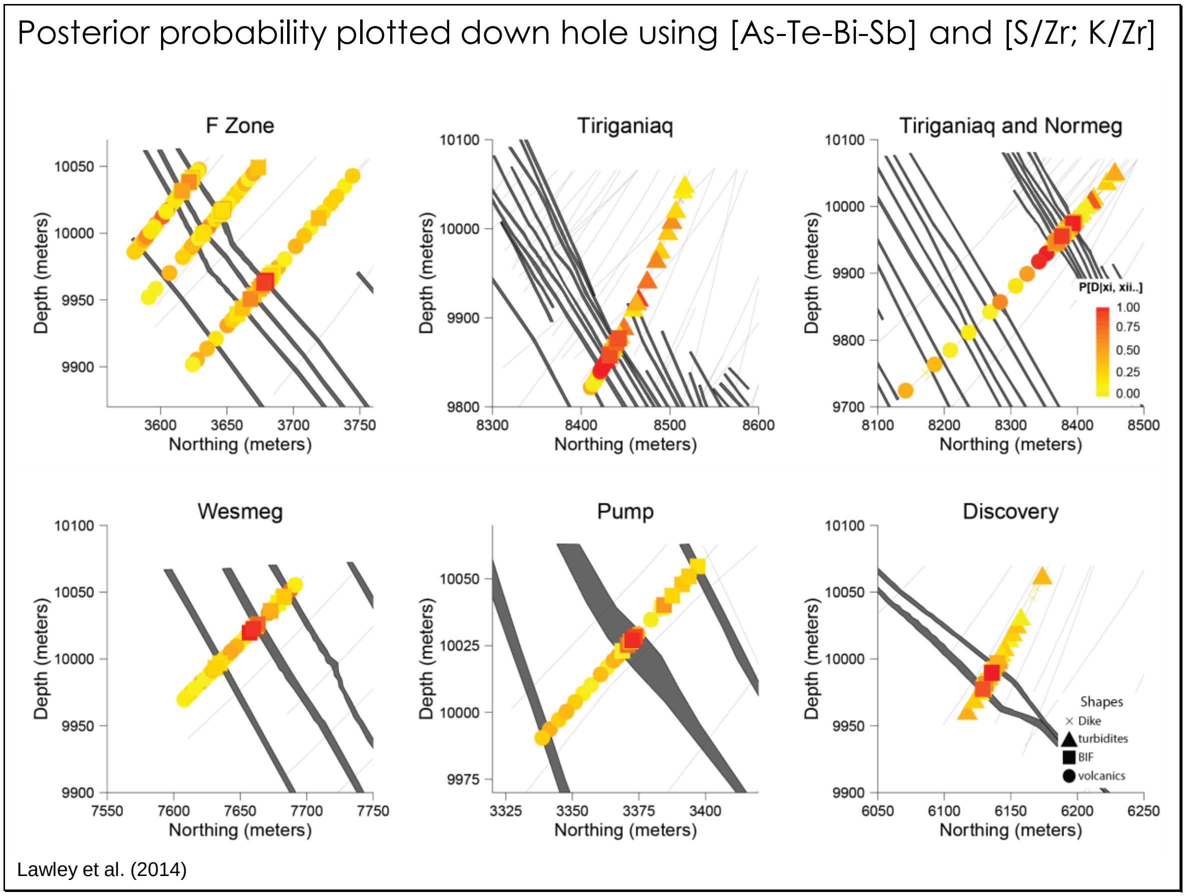

Posterior probabilities plotted down hole and calculated as a function of pathfinder element enrichment (As-Te-Bi-Sb) and hydrothermal alteration (simple PERs; S/Zr; K/Zr). The maps highlight the probability of each sample being mineralized given the simultaneous occurrence of multi-path finder element enrichment and hydrothermal alteration. However, absolute posterior probabilities are strongly dependent on the assumption of conditional independence, which in this case is invalid (Cheng and Agterberg, 1999). As a result, absolute posterior probabilities are likely overestimated; whereas relative changes in posterior probabilities are still likely significant.

Slide 16

The fuzzy footprint approach provides a framework to address samples that are transitional between barren and mineralized end-members. These transitional samples are difficult to classify using field observations and compliment many current exploration core-logging programs that address this issue by dividing samples into qualitative classes e.g., least altered, moderately altered, extremely altered; and non-, weak and strongly-mineralized. We emphasize that absolute posterior probabilities are likely overestimated due to the violation of the conditional independence assumption.

Slide 17

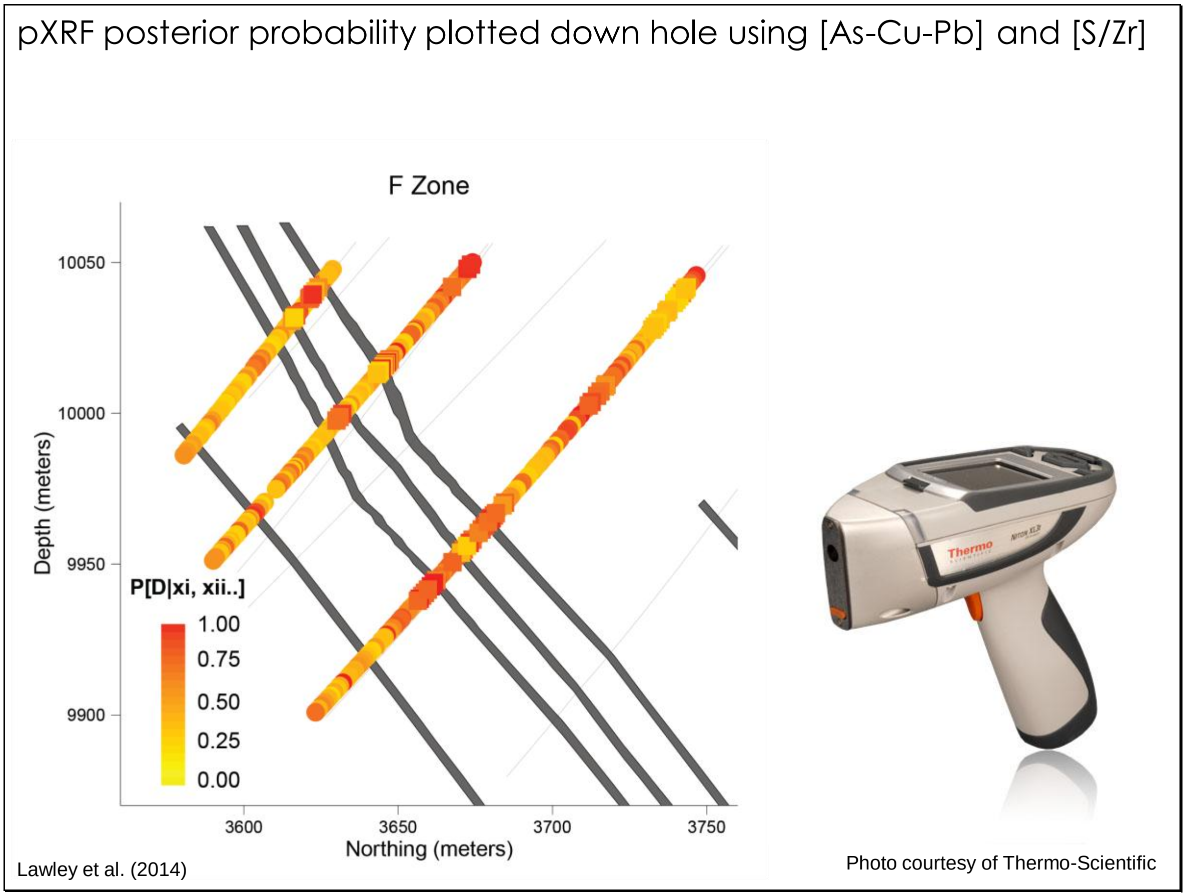

Posterior probability, for pXRF data, plotted down hole. Fuzzy WofE were selected to reflect elements (As, Cu, Pb, S/Zr) that are routinely collected via pXRF.

Slide 18

Conclusions

(1) BIF-hosted gold deposits are enveloped by multivariate footprints

(2) Hydrothermal footprint extends 10s to 100s of meters beyond high-grade ore and into hanging wall and footwall rocks devoid of gold (<5 ppb Au)

<u>AND</u>

(3) Major benefits to accommodating uncertainty and following a multivariate approach for fuzzy footprint mapping.

Natural Resources Canada | Ressources naturelles Canada

Canada

Slide 19

Acknowledgements and references

AGNICO EAGLE

TGI 4 Ore Systems

All data handling and plots were completed in R.

ggplot2 for plotting
Wickham, H., 2009. ggplot2: Elegant graphics for data analysis. Springer New York. 213 p.

robCompositions for data handling
Templ, M., Hron, K., and Filzmoser, P., 2010. robCompositions: Robust estimation for compositional data. Manual and package, version 1.3.3.

Fuzzy Weights of Evidence protocol followed: Cheng, Q., and Agterberg, F.P., 1999. Fuzzy weights of evidence method and its application in mineral potential mapping. Natural Resources Canada, v. 8, p. 27–35.